Discovery, engineering, and applications of amino acid and peptide prenyltransferases

Florian Hubrich [*] [abc]

Covering: up to 2025

Amino acid and peptide prenylation leads to a large variety of natural products, including neurotoxins, alkaloids and (non-)ribosomal peptides, with potent bioactivities. The key biosynthetic enzymes are structurally diverse prenyltransferases, which attach short, linear prenyl donors to amino acid acceptor substrates, and show impressive regio- and chemo-selectivity. The emerging number of characterized prenyltransferases, along with their scope, promiscuity, and engineering, provides an expanded chemoenzymatic toolbox for amino acid prenylation and peptide late-stage functionalization with potential in industrial applications such as peptide-based drug development.

1 Introduction

Prenyltransferases (PTs) are key enzymes in primary and secondary metabolism across many biological processes. They catalyse the transformation of isoprenoid donors with different chain lengths to a variety of electron-rich acceptor substrates.[1] In primary metabolism, protein prenylation of cysteine residues with farnesyl pyrophosphate (FPP, C_{15}) or geranylgeranyl pyrophosphate (GGPP, C_{20}) is an important post-translational modification, playing crucial roles in protein–protein interactions and protein localization at cellular membranes.[2] In addition, the essential electron carriers ubiquinone and menaquinone are prenylated metabolites.[3]

In secondary metabolism, prenylation is found in all natural product (NP) superfamilies, with alkaloids,[4] non-ribosomal peptides (NRPs),[5] and ribosomally synthesized and post-translationally modified peptides (RiPPs)[6] sharing amino acids (AAs) as acceptor substrates for short, linear prenyl donors such as dimethylallyl pyrophosphate (DMAPP, C_5), geranyl pyrophosphate (GPP, C_{10}), FPP, and GGPP. The acceptor substrates range from free AAs[5] and cyclodipeptides[7] to larger ribosomal peptides.[8] The free AAs that are known to be prenylated are Trp,[5] Tyr,[4] His,[9] Arg,[10] and Glu.[11] Electron-rich AA residues prenylated in di- and poly-peptides include the aforementioned Trp,[7] Tyr,[12] His,[13] and Arg[14] as well as Ser,[15] Thr,[16] and the peptide C- and N-termini.[17]

The ability of PTs to regioselectively target distinct free AAs and AA residues makes them promising tools for chemoenzymatic peptide functionalization, with advantages over synthetic prenylation. Although efficient synthetic methods have been developed, they rely on metal catalysis, toxic reagents and halogenated solvents.[18] In addition, isoprenoid moieties installed in peptides during synthesis are often acid-labile and highly reactive due to the presence of alkene groups, limiting opportunities for protection strategy, resin cleavage, and follow-up chemistry, resulting in a drop in overall yield. Peptide late-stage functionalization, in particular, the mild conditions of chemoenzymatic prenylation,[19] overcome these challenges.[20]

Overall, PTs facilitate the incorporation of lipophilic moieties in peptides during drug development, promoting positive effects on physicochemical, pharmacokinetic and pharmacodynamic properties and overcoming the typical challenges of peptide drugs such as low oral bioavailability, quick renal clearance, and rapid proteolytic digestion.[21] Moreover, prenylation improves or induces bioactivities in peptide NPs and peptides of synthetic origin.[22,23]

In this review, an overview of the progress in the emerging field of AA and peptide PTs is given. By presenting an overview of the different enzyme families and selected (recent) examples to showcase the value of PTs for chemoenzymatic synthesis of prenylated peptides and their application in drug development, this review article aims to emphasise key advances in the field and outline its future directions and untapped potential.

2 The impact of prenylation on natural product bioactivity

Prenylated NPs show a large variety of reported bioactivities, including anticancer,[6] antiplasmodial,[5] and antibacterial activities.[14] Prenylation often improves or induces the bioactivity of

aDepartment of Pharmacy, Saarland University, Campus C2.3, 66125 Saarbrücken, Germany. E-mail: florian.hubrich@uni-saarland.de

bNatural Products of underexplored pathways and extreme environments, Helmholtz Institute for Pharmaceutical Research Saarland (HIPS), Helmholtz-Centre for Infection Research (HZI), Campus E8.1, 66125 Saarbrücken, Germany. E-mail: florian.hubrich@helmholtz-hips.de

cPharmaScienceHub (PSH), Saarland University, Campus E2.1, 66125 Saarbrücken, Germany

This journal is © The Royal Society of Chemistry 2026

Nat. Prod. Rep., 2026, **43**, 415–426 | 415

NPs by increasing hydrophobicity, membrane interaction, or metabolic stability.

Prenylated AAs are further biosynthesised to produce potent neurotoxins, protease inhibitors and bioactive alkaloids. Domoic acid (Fig. 1) and kainic acid are neurotoxins that are harmful for mammals;[11] they are produced during algal blooms and control environmental food webs. *N*-Prenylation of Glu represents the initial step of their biosynthesis. Aeruginosins and aeruginoguanidines (Fig. 1) are protease inhibitors and cytotoxic peptides,[10,24] respectively, containing *N*-prenylated agmatine and Arg. In addition, *O*-prenylation of Tyr and subsequent biosynthetic steps lead to the formation of the phytotoxin sirodesmin PL (Fig. 1).[4]

Important examples of bioactive prenylated NRPs include the structurally related cyclomarins (Fig. 1),[5] rufomycins,[25] and metamarins,[26] isolated from marine Actinomycetes, sharing an *N*-prenylated Trp in their cyclic structure. They are potent antibacterial compounds against *Mycobacterium tuberculosis*. In addition, cyclomarins and rufomycins are antimalarial agents.[25] Moreover, indolactam V-derived cyclic dipeptides, as exemplified by the reverse *C*-geranylated lyngbyatoxins (Fig. 1) and teleocidins, exhibit tumor-promoting activity.[27] In contrast, prenylated cyclic dipeptides of the diketopiperazines (DKPs) include the cytotoxic fungal DKP tryprostatins,[28] and the pyrroloindoline-containing antiviral lansais (Fig. 1).[22] For both DKPs, indole *C*-prenylation is essential for their bioactivity.[22,28]

Bioactive prenylated ribosomal peptides have numerous examples in the cyanobactin RiPP family, such as the antibacterial muscoride A (Fig. 1)[17] and argicyclamides,[14] as well as the cytotoxic patellamides, including the former antitumor drug candidate trunkamide A (Fig. 1).[6] In contrast, the farnesylated or geranylated ComX peptides (Fig. 1) from different *Bacillus subtilis* play an ecological role as hormones.[29]

Despite the versatile bioactivities reported for prenylated NPs, the number of studies investigating structure–activity relationships (SARs) and modes of action for prenylated NPs is limited. However, there are synthetic and semi-synthetic approaches to tackle these important questions for drug development. Kazmaier and co-workers established a total synthesis approach to dozens of cyclomarin-derivatives with variations at different chemical moieties. These cyclomarin-derivatives enabled detailed SAR studies, showcasing that prenylation plays a key role for cyclomarin bioactivity. However, it was also shown that smaller alkyl groups, such as indole *N*-methylated Trp, retain bioactivity.[30]

In contrast, Ozawa *et al.*[23] used chemoenzymatic prenylation with the PT PalQ to improve the bioactivity of synthetic antimicrobial peptides (AMPs) against pathogenic bacteria. The ratio between improved bioactivity and unwanted cytotoxicity was superior when compared with the ratio for the corresponding fatty acylated AMP. This study added to recent observations indicating that peptide prenylation improves antibacterial bioactivity without increasing the cytotoxicity against mammalian cells to an extent that causes failure during pre-clinical development.[31]

3 Substrate scope and enzyme classes

PTs act on a broad range of substrates, including free AAs, dipeptides, and ribosomal peptides. Different soluble and membrane-bound PT families adopt several structural folds, with the majority belonging to the all α-helical isoprenyl diphosphate synthase (IDS)-like family and the so-called ABBA-type family (Fig. 2);[32,33] the ABBA-fold PTs share a β-barrel, formed by ten antiparallel β-sheets decorated with two α-helices, harbouring the active site in a central cavity. Loops covering the active site in AA and DKP ABBA-type PTs are likely responsible for their small substrate selectivity by shielding the formed carbocation from solvent quenching.[34] In addition, the position and flexibility of the loops are important for the promiscuity towards peptide substrates.[35] The loops are missing in ABBA-type PTs utilizing RiPPs, such as the cyanobactin PTs (Fig. 2), where the peptide substrate covers the active site instead.[36] Depending on the PT family, they are promiscuous or rigid in their donor and acceptor selectivity, including non-natural representatives, opening a plethora of opportunities for synthetic and medicinal applications (see the following two sections). This section will highlight examples across acceptor substrate classes, moving from AA PTs to peptide-modifying PTs.

3.1 Amino acid prenyltransferases

PTs acting on AAs are commonly found in biosynthetic gene clusters encoding for alkaloid[4] and NRP production.[5] They mainly belong to the soluble aromatic PTs but also include enzymes with structural similarity to other PT folds (Fig. 2). These enzymes highlight the versatility of prenylation in generating structural diversity from simple precursors.

3.1.1 ABBA-fold PTs. The ABBA-fold PTs acting on AAs are enzymes from the dimethylallyl Trp synthase (DMATS) family, found in bacteria and fungi. Well-characterized members include the bacterial DMATS CymD (Fig. 2)[5] and PriB,[31] as well

Florian Hubrich studied Chemistry and Biology at the University of Freiburg (Germany) and completed his PhD in 2014 under the supervision of Prof. Jennifer Andexer and Prof. Michael Müller. Afterwards, he worked at Bachem AG as a Project Chemist and Group Leader. In 2019, he joined Prof. Jörn Piel's lab at ETH Zurich as a Postdoctoral Researcher, studying RiPP biosynthesis. In 2024, he established his junior research group at the Helmholtz Institute for Pharmaceutical Research Saarland and the Saarland University, focusing on expanding prenylated peptide diversity for drug development and characterising biosynthetic enzymes from underexplored pathways.
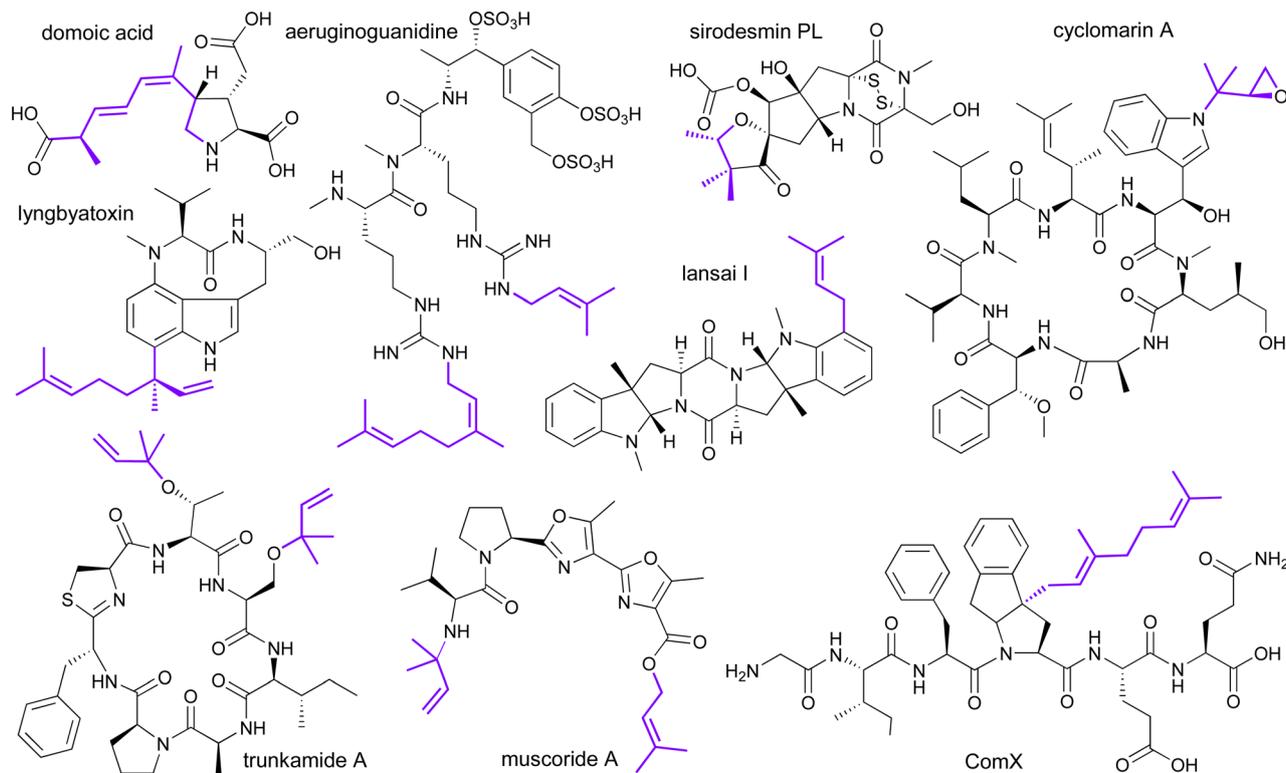
Florian Hubrich

Fig. 1 Prenylated bioactive NPs: domoic acid (monomer AA; Glu forward *N*-geranylation), aeruginoguanidine A (NRP; Arg forward *N*-prenylation/-geranylation), sirodesmin PL (alkaloid; Tyr forward *O*-prenylation), cyclomarin A (NRP; Trp reverse *N*-prenylation), lyngbyatoxin A (NRP; dipeptide reverse *C*-geranylation), lansai I (DKP; dipeptide reverse *C*-prenylation), trunkamide A (RiPP; peptide reverse *O*-prenylation), muscoride A (RiPP; reverse N-terminal and forward *C*-terminal prenylation) and ComX (RiPP; peptide forward *C*-geranylation).

as fungal 7-DMATS[37] and FgaPT2,[38] providing a variety of regio- and chemo-selectivity at the indole ring (Fig. 3). Despite their family name, DMATS members also include characterized members that prenylate other aromatic AAs; for example, SirD catalyses forward *O*-prenylation of Tyr with DMAPP (Fig. 3).[4]

Recently, Chen *et al.*[9] characterized FunA, the first PT using l-His as the native substrate, during the biosynthesis of the antifungal NP fungerin. FunA catalyses forward *C*-prenylation at C4 of the His imidazole ring (Fig. 3). Structural studies on DMATS were recently comprehensively reviewed by Miller, Tsodikov and Garneau-Tsodikova.[35] Elucidation of FunA's three-dimensional structure and Ala scanning of the active site residues provided a detailed understanding of the regio-selectivity for the C4 position.[9] Comparison with other DMATS structures highlighted the conservation of important prenyl donor binding motifs and key residues for proton abstraction during catalysis, independent of the AA's nature.

3.1.2 IDS-like PTs. All IDS-like PTs that utilize AAs as native substrates specifically prenylate Arg and the Arg derivative agmatine. Very recently, Ikuro Abe and co-workers characterized one agmatine-specific PT, ScAer3, and two Arg-specific PTs, AgdS and AgdT, all from cyanobacterial origin. ScAer3 catalyses the forward *N*-prenylation of agmatine at the internal N4 of the guanidino moiety.[10] In contrast, AgdS and AgdT tolerate both agmatine and Arg as acceptor substrates, but the preferred prenyl donor is GPP (Fig. 3). Structural models suggest similarity to all α-helical IDS (Fig. 2), such as CyS, but the sequence

motifs responsible for magnesium ion and prenyl donor binding are distinct. Another predicted IDS-like PT is GroH, which is involved in the biosynthesis of the pentacyclic triterpene NP gromomycin.[39] Feeding experiments and gene deletion of *groH* enabled a postulate of the gromomycin biosynthesis, involving prenylation at the guanidino N2 of Arg with hexaprenyl-PP (Fig. 3), and proline as a leaving group, to form linear hexaprenylguanidine, which is subsequently cyclized.

3.1.3 Terpene cyclase-fold PTs. A unique structural fold that revealed PT-activity is represented by an algal enzyme family catalysing the *N*-prenylation of the Glu's primary amine in domoic and kainic acid biosynthesis (Fig. 3).[11] Both enzymes employ different prenyl donors: DabA is GPP-specific and KabA is DMAPP-specific. The DabA structure shows a terpene cyclase-like fold with similarity to the selinadiene synthase, but the all α-helical structure shows insertions in the core structure and an N-terminal extension, both including β-hairpins (Fig. 2). This demonstrates how nature has evolved entirely new structural scaffolds for prenylation by reshaping a canonical active site for fundamentally different chemistry. The active sites of DabA and KabA form a narrow channel, which hinders terpenoid cyclisation but stabilises the carbocation for prenylation.

3.2 Dipeptide prenyltransferases

PTs that modify dipeptides mostly act on DKPs; the key biosynthetic machinery establishing the core scaffold is either a tRNA-

This journal is © The Royal Society of Chemistry 2026

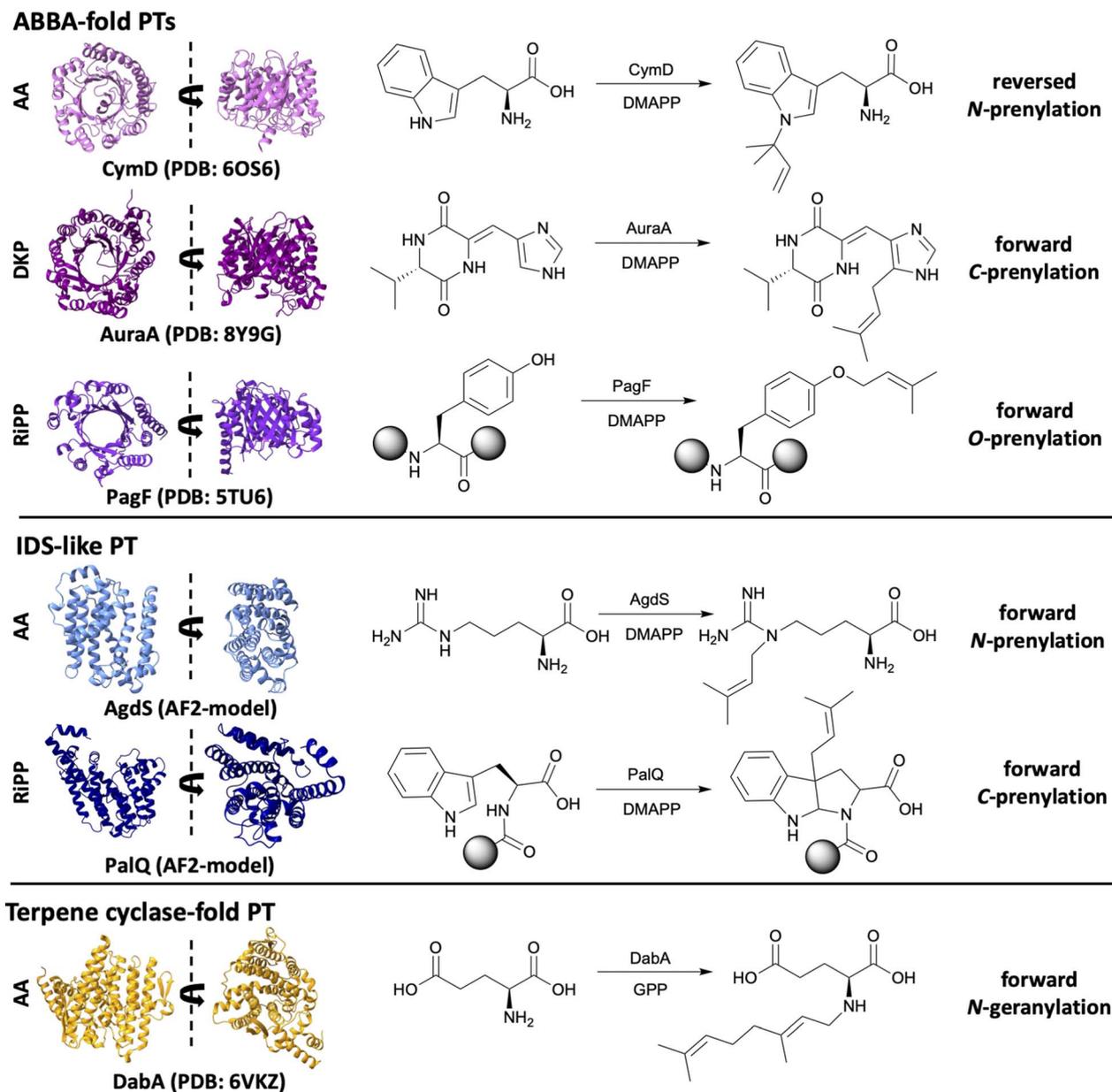*Nat. Prod. Rep.*, 2026, **43**, 415–426 | **417**

Fig. 2   AA and peptide PT structural folds, and the reactions catalysed by PTs. Experimentally determined ABBA-fold PTs (purple) include representatives from the DMATS (CymD, AuraA), and cyanobactin PT family (PagF). IDS-like PTs (blue) are predicted structures from ref. 10 (AgdS) and ref. 23 (PalQ), while a single experimentally determined structure was obtained from the terpene cyclase-like PTs (yellow, DabA).

dependent cyclodipeptide synthase (CDP) or an NRP synthetase (NRPS). The PT-fold often correlates with the biosynthetic origin, reflecting the convergent evolution of DKP prenylation.

3.2.1   tRNA-dependent DKP PTs. The prenylated DKPs from tRNA-dependent CDP biosynthetic origin all contain at least a Trp residue that forms a pyrroloindoline-containing scaffold;[22] it is formed during the prenylation process or additional tailoring, *e.g.*, methylation. Six bacterial IDS-like PTs with similarity to phytoene synthases are characterized, leading to a large structural diversity. Four PTs are specific for C3/C3′ prenylation, including DmtC (L-Trp/L-Xaa, FPP-specific),[40] NozPT (D-Trp/D-Trp, DMAPP-specific),[41] GczB (L-Trp/L-Trp, DMAPP-specific),[42] and SazB-PT (L-Trp/L-Trp, DMAPP-specific; Fig. 3), with SazB being a bifunctional enzyme

featuring a PT and a methyltransferase domain.[43] In griseocazine biosynthesis, an additional PT GczC prenylates specifically C3-prenylated L-Trp/L-Trp at C2′ or C3′ with relaxed prenyl donor specificity (DMAPP, GPP, and FPP; Fig. 3).[42] Very recently, LanB was characterized as a bis-pyrroloindoline-specific PT, attaching prenyl moieties at C5′ or C7′ in the reverse or forward direction, respectively (Fig. 3).[22] Finally, the structural diversity of farnesyl moieties attached by DmtC is increased by the terpene cyclase DmtA, which installs bicyclic terpenoid moieties.[40] The dual role in prenylation and downstream cyclization makes the drimentine biosynthetic enzymes interesting candidates to develop as biocatalysts.
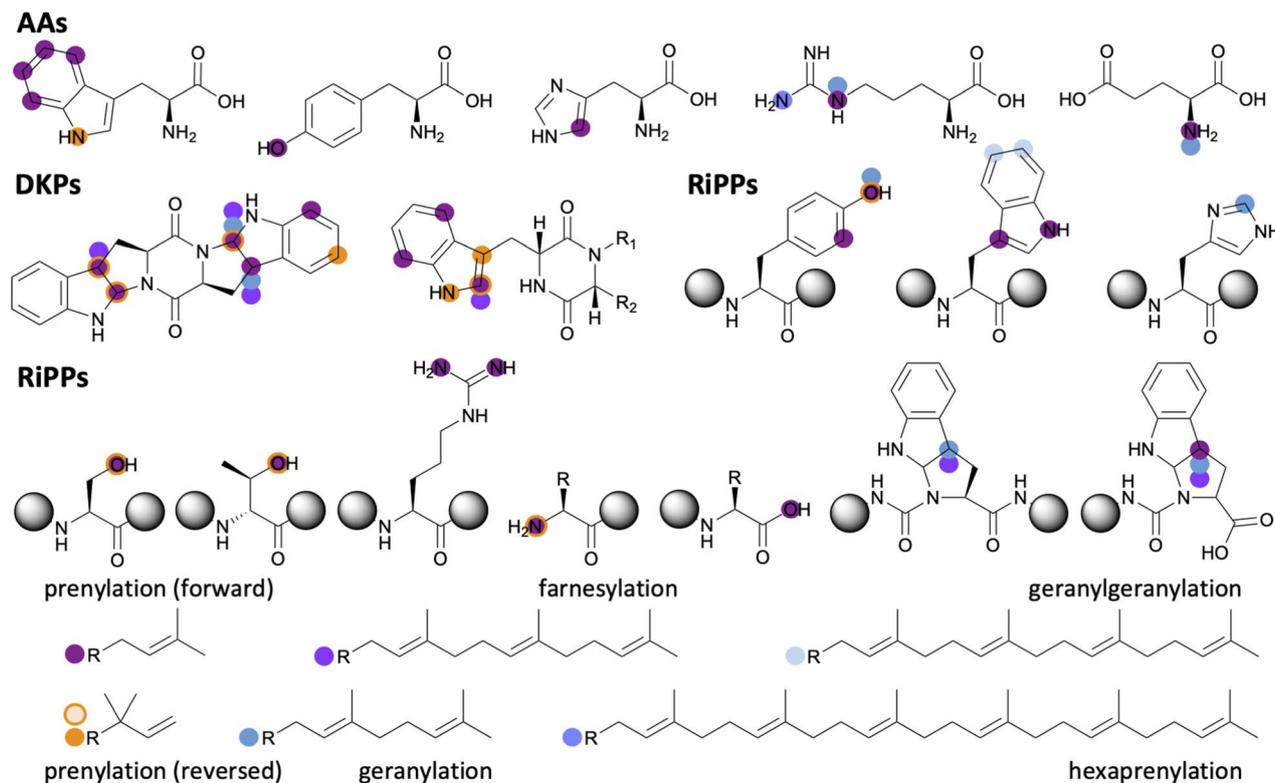
418 | *Nat. Prod. Rep.*, 2026, **43**, 415–426

This journal is © The Royal Society of Chemistry 2026

Fig. 3 Regio- and chemo-selectivity of native prenylation reactions. Multiple circles at a specific position indicate prenyl donor promiscuity. Orange rings surrounding coloured circles indicate that forward and reverse prenylation with the respective prenyl donor has been reported.

3.2.2 NRPS-derived DKP PTs. In contrast to the IDS-like PTs associated with tRNA-dependent CDP, NRPS-derived DKPs are associated with ABBA-type PTs, mostly from fungi. They utilize DMAPP as a prenyl donor in forward and reversed fashion at different positions of the Trp indole ring, including C2, C3, C4, C7 and N1 (Fig. 3). Although their full diversity has been comprehensively reviewed,[35,44,45] prominent examples are NotF[7] and CdpNPT from *Aspergillus* species.[46] Recently, the membrane-bound UbiA-type PT FtaB, identified by targeted genome mining, was characterized.[47] FtaB farnesylates the C2 of the indole ring from indolyl DKP with Gly, norvaline, D-Val and L-Pro. The latest example, AuraA from *Penicillium solitum*, shows DMAPP-specific reverse C5 imidazole ring prenylation of the DKP L-Val/dehydrohistidine, leading to aurantiamine (Fig. 2).[13]

In summary, fungal ABBA-type DKP PTs are notable for their remarkable acceptor substrate promiscuity, which enables the generation of pharmacologically relevant molecules, as will be discussed in the next sections.

3.2.3 Indolactam V PTs. A subset of bacterial ABBA-fold PTs act on indolactam V, a cyclic dipeptide of Trp and *N*-Me-Val.[27] Enzymes, such as the cyanobacterial LtxC, as well as TleC and MpnD from *Streptomyces*, catalyse reverse C7-geranylation of the indolactam V indole, displaying relaxed donor specificity from DMAPP up to GGPP.

3.3 RiPP prenyltransferases

RiPPs represent an emerging NP superfamily.[48] RiPP biosynthesis relies on precursor peptide production at the ribosome;

the leader region of the precursor often represents a recognition element for modifying enzymes that install post-translational modifications in the core region. Both ABBA-type and IDS-like PTs have been characterized in the context of RiPPs; some representatives form fusion proteins with terpene cyclases. These enzymes rapidly expanded the chemical space of prenylated RiPPs.

3.3.1 Cyanobactin PTs. Cyanobactin PTs are the largest and best characterized family of RiPP PTs. They catalyse leader-independent prenylation (forward and reversed) and geranylation (forward) at Tyr,[36,49] Trp,[50,51] His,[52] Ser,[15] Thr,[16] and Arg,[14] and the C- and N-termini of linear and cyclic peptides (Fig. 3).[17] In total, 18 cyanobactin PTs are characterized today, two of them are reported to be inactive. Cyanobactin PT group into clades in sequence similarity networks along their AA substrate specificity, facilitating prioritization for biochemical studies. However, the underlying prenyl donor selectivity will remain elusive until an NP is isolated or the PT is biochemically characterized. Cyanobactin PTs were recently reviewed in detail by working groups that have made important contributions to the field,[34,53] highlighting examples and developments that showcase the value of cyanobactin PTs as chemoenzymatic tools for peptide late-stage functionalization. Important characterized cyanobactin PTs include TruF, which catalyses reversed *O*-prenylation of Ser and Thr.[15] In addition, KgpF and AcyF share Trp as the acceptor substrate for forward *C*- and *N*-prenylation, respectively.[50,51] Moreover, PagF uses DMAPP for forward *O*-prenylation of Tyr (Fig. 2),[36] while the bifunctional AgeMTPT

This journal is © The Royal Society of Chemistry 2026

Nat. Prod. Rep., 2026, **43**, 415–426 | 419

attaches DMAPP in the reverse direction at the N-terminus of linear peptides.[54] In contrast, Zhang et al. characterized the GPP-specific PT LimF,[52] the only characterized cyanobactin PT accepting two different AA substrates with distinct chemoselectivity: His C-geranylation and Tyr O-geranylation. Very recently, Wakimoto and colleagues characterized DciF, catalysing N-bisprenylation of Arg (Fig. 3).[55] Structure elucidation of DciF revealed the active-site residue responsible for bis-versus mono-prenylation.

3.3.2 IDS-like RiPP PTs. In 2005, ComQ from *Bacillus subtilis* was the first RiPP PT postulated,[29] catalyzing species-specific C-prenylation of Trp residues with GPP or FPP during ComX biosynthesis (Fig. 3).[56] More recently, a combination of genome mining and AlphaFold2-guided structure prediction enabled the characterization of PalQ from *Paenibacillus alvei*.[57] The predicted structure suggested an IDS-like PT-fold (Fig. 2), and sequential alignment suggested that, in contrast to ComQ, both aspartate-rich motifs responsible for magnesium ion and prenyl donor binding are present in PalQ. In addition, the PT was found to prenylate specifically the C-terminal Trp of its precursor peptide PalX, with multiple donor substrates (DMAPP, GPP and FPP; Fig. 3) generating a pyrroloindoline moiety.

3.3.3 PT-terpene cyclase fusions. Finally, Hubrich et al. characterised two hybrid enzymes that fuse distinct PTs with homologs of the monodomain terpene cyclase MstE.[8] The PT domain of the cyanobacterial PT-terpene cyclase fusion enzyme NctPC was predicted to adopt an ABBA-type fold, which is distinct from the crystal structures of DMATS and the cyanobactin PT family. In contrast, ChrPC from *Chryseobacterium tenax* has a predicted IDS-like PT domain. Both enzymes catalyse C-geranylgeranylation of Trp (Fig. 3) at the indole C5 or C6, followed by cyclization into pseudo-steroid scaffolds, generating unprecedented NP architectures.

4 Promiscuity, engineering, and application of peptide prenyltransferases

AA and peptide PTs vary widely in their natural promiscuity. Understanding the structural basis of how these enzymes catalyse prenyl transfer has enabled engineering strategies to expand enzyme specificity, selectivity, and scope. In addition, the application of PTs in chemoenzymatic synthesis generates structurally novel and bioactive peptides that are useful for drug development.

4.1 Substrate and donor promiscuity of peptide PTs

ABBA-type PTs are often specific for a single AA, but relaxed regarding the surrounding AA sequence, leading to promiscuous enzymes that accept a variety of peptide substrates. In contrast, they frequently show a strong preference for a single native prenyl donor, mostly DMAPP, as exemplified by the cyanobactin PTs,[34] but high promiscuity towards non-natural prenyl donors.[58]

The Tyr PTs, TyrPT and SirD, showed promiscuity towards twelve non-proteinogenic AAs, in combination with DMAPP, MAPP, 2-pentenyl-PP, and benzyl-PP, ranging from full conversion to trace amounts;[59] SirD also accepts Phe and Trp derivatives as substrates.[60]

Three representatives from the DMATS family, PriB, FgaPT2, and CdpNPT, showcase how enzymes utilizing Trp and indole-DKP as native substrates exhibit remarkable promiscuity towards large peptides, such as the FDA-approved antibiotic daptomycin (Fig. 4).[31,46,61] In addition, the enzymes revealed a remarkable promiscuity for a large panel of synthetic alkyl donors with their native substrates, as well as larger peptides.

Another very promiscuous DKP PT is NotF, installing a reverse prenyl moiety at the C2-position of the indole ring on brevianamide F.[7] The substrate scope of NotF was expanded to 30 tryptophanyl DKP derivatives, providing chemoenzymatic access to indole alkaloid key intermediates and NPs (Fig. 4). Moreover, AuraA catalyses forward C2-prenylation instead of reverse C5-prenylation when the DKP L-Val/L-His is the substrate.[13]

Cyanobactin PTs are very relaxed regarding peptide substrates, often with a preference for cyclic peptides if the native substrate is cyclic as well.[16,49,50,52,55] Despite their flexibility for peptide substrates, they often poorly or do not prenylate free AAs and small molecules.[16,49,50] The most striking examples illustrating the remarkable promiscuity of cyanobactin PTs are the His C2-PT LimF and the Trp C3-PT KgpF.[52,62] Both accept a huge diversity of thioether macrocyclic peptides (teMP) produced by the random nonstandard peptide integrated discovery (RaPID) platform. Furthermore, LimF was shown to prenylate FDA-approved bioactive peptides containing imidazole moieties, such as leuprorelin (Fig. 4).[52] Although cyanobactin PTs are typically specific for a single natural prenyl donor,[63] there is a study that explored the promiscuity of AcyF, testing 22 alkyl pyrophosphate donors, of which six were accepted.[58]

In contrast, IDS-like PTs are often flexible toward different natural prenyl donors, but more constrained in peptide recognition. Nevertheless, the PalQ showed prenylation of eight synthetic AMPs containing a C-terminal Trp (Fig. 4);[23] among those, three were only accepted as engineered versions, showing at least one Gly in front of the C-terminal Trp.

In summary, these case studies highlight the promiscuity of peptide PTs. They accept a variety of non-natural peptide substrates and unusual alkyl donors, illustrating their potential for chemoenzymatic applications, such as peptide late-stage functionalization.

4.2 Engineering of peptide PTs

Numerous studies have reprogrammed PTs for altered specificity or selectivity. These efforts have achieved shifts in acceptor and switches in prenyl donor specificity, improvements in activity, and changes in regioselectivity.

4.2.1 Peptide substrate engineering. Studies aimed at peptide substrate engineering have mainly focused on ABBA-type PTs of the DMATS family. Site-directed mutagenesis has expanded the substrate scope by rational enzyme design and saturation mutagenesis, predominantly performed in the lab of
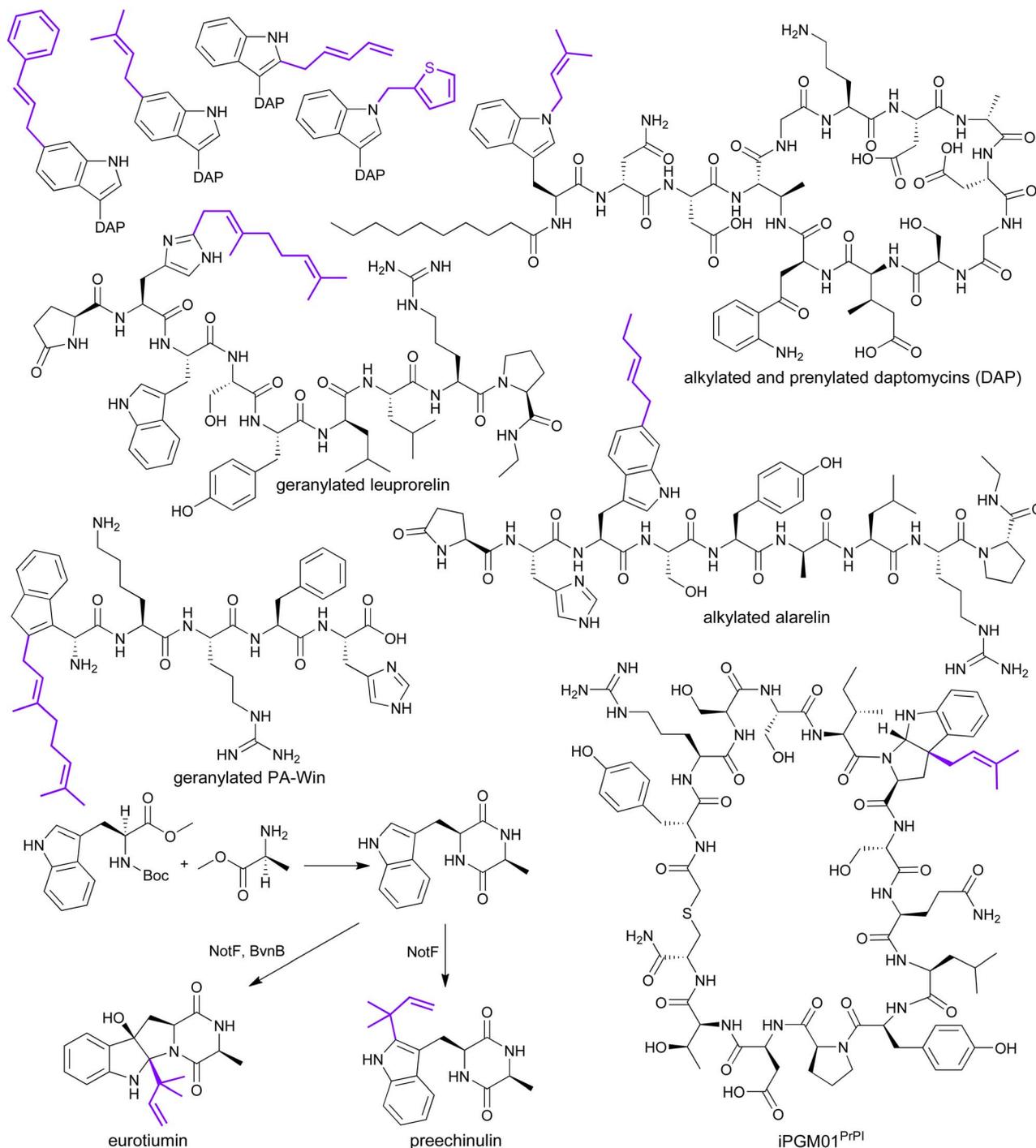
420 | *Nat. Prod. Rep.*, 2026, **43**, 415–426

This journal is © The Royal Society of Chemistry 2026

Fig. 4 Selected examples of bioactive peptides from synthetic and NP origin, allowing chemoenzymatic peptide late-stage functionalization, including FDA-approved drugs. The regio- and chemo-selectivity exhibited by different native and engineered AA and peptide PTs highlight the structural diversity accessible with natural and non-natural prenyl- and alkyl-PP donors. Selected examples of prenylated and alkylated dap-tomycin derivatives from ref. 31, 46, and 61; geranylated leuprorelin from ref. 52; geranylated plantaricin A C-terminal mimic (PA-Win) from ref. 23, alkylated alarelin from ref. 69; and prenylated iPGM01[PrPl] from ref. 62. The reaction at the bottom left shows the chemoenzymatic synthesis of preechinulin and eurotiumin A via two- and three-step total syntheses, as shown in ref. 7.

Shu-Ming Li.[44] Moreover, engineering of the AA PT FgaPT2, catalysing l-Trp forward C4-prenylation, provided the variant FgaPT2[Lys174Phe], which showed much higher specificity towards l-Tyr C3-prenylation.[64] In contrast, saturation mutagenesis of FgaPT2 at Arg244 led to thirteen FgaPT2 variants with increased

turnover numbers for indole DKPs.[38] The activity was further boosted by combining both residues in the respective double variants.[64]

The variant AuraA[Tyr207Ala] resulted in forward C5-prenylation of the DKP L-Val/dehydrohistidine, providing access to the

fungal NP viridamine.[13] Induced fit docking-guided engineering of NotF revealed three active site residues, where the decrease of steric hindrance of NotF variants increased reaction rates of two tryptophanyl DKPs with an additional aromatic residue.[7] In contrast, the native reversed C2-prenylation of brevianamide F was almost abolished by these NotF variants.

Engineering of RiPP PTs is less advanced. However, work on the IDS-like PT PalQ underlines the promise of stability and activity tuning, using bioinformatic-guided optimization, enabling geranylation of AMPs that are otherwise poorly accessible or inaccessible by the native enzyme.[23]

Finally, engineering of the LimF binding pocket, by introducing the point mutation Ile52Ala, further broadened the substrate tolerance of LimF for non-natural peptide substrates.[65] In contrast, AgeMTPT^{Tyr263Leu} expanded the substrate scope to a heptapeptide that was formerly not prenylated, but with reduced reaction rate, while the reaction rate for the native peptide substrate significantly increased.[66]

4.2.2 Donor engineering. Experimentally determined crystal structures and *in silico* modelling have enabled the rational design of prenyl donor binding pockets. Thereby, the donor specificity was shifted or expanded, typically from DMAPP to larger donors, like GPP or FPP.

Structure-guided mutations of FgaPT2 shifted the prenyl donor preference from DMAPP to GPP for variants where Met328 was exchanged for small AAs, such as Gly, Ser or Ala, while aromatic AAs instead of Met328 caused DMAPP-specific FgaPT2 variants.[67] These results highlight that Met328 is the gatekeeper for the prenyl donor binding pocket in FgaPT2.

A similar observation was noted for the structurally unrelated terpene cyclase-like PTs KabA and DabA.[11] Here, elucidation of the three-dimensional structure of DabA and homology-based modelling of KabA showed that DabA^{Thr134} (KabA^{Met114}) determines prenyl donor specificity by controlling the size of a hydrophobic tunnel. The prenyl donor specificities of both enzymes were interchanged by introducing the corresponding AA residue into the respective enzyme variant.

Intensive efforts to change the donor specificity of cyanobactin PTs have been made over the last decade. First, comparison of the active sites from the Tyr PTs PagF and PirF showed a single AA difference that was expected to be responsible for prenyl donor specificity.[36,68] This assumption was proven correct with the variant PagF^{Phe222Gly}, causing a switch in donor specificity from DMAPP to GPP.[68] The corresponding variant AgeMTPT^{Gln215Gly} geranylated the native heptapeptide substrate of AgeMTPT quantitatively.[66] Inspired by these results, Zhang *et al.* achieved the structure-guided engineering of LimF from GPP-specificity to DMAPP-specificity (LimF^{Gly224Met}).[63] Additional Ala scan and saturation mutagenesis, together with rational enzyme design, established the FPP-specific double variant LimF$^{His239Gly/Trp273Gln}$. The obtained results were then used to engineer the triple variant PagF$^{Phe222Gly/His237Gly/Trp271Gln}$, with enhanced FPP activity, by changing the corresponding positions of the LimF residues responsible for donor specificity. Very recently, the crystal structure of DciF revealed the structural basis of Arg *N*-bisprenylation in cyanobactin PTs.[55] Comparison of the DciF active site with an AlphaFold

model of AutF, catalysing Arg forward *N*-monoprenylation, identified Asp65 in AutF that could potentially exclude monoprenylated products as substrates for additional forward *N*-prenylation. The hypothesis was confirmed by the two variants DciF^{Gly65Leu} and AutF^{Asp65Gly}, where the ability for mono- and bis-prenylation was switched when compared to the wildtype enzymes.

Finally, structural modelling broadened the prenyl donor specificity of PalQ by enlarging the active site pocket with a quadruple variant.[23] This variant accepted GGPP as a prenyl donor, in addition to DMAPP, GPP, and FPP, for the prenylation of the native substrate PalX.

4.3 Applications of peptide PTs

The natural and engineered promiscuity of PTs enables a wide range of applications in chemoenzymatic synthesis of NP derivatives and peptide late-stage functionalization of (bioactive) peptides.

The broad substrate scope of the fungal PT NotF enabled the first total synthesis of the DKP NP (−)-eurotiumin A over three steps, with 60% yield (Fig. 4).[7] The last step was a chemoenzymatic telescope reaction, using a two-enzyme cascade of NotF and the monooxygenase BvnB.

Promiscuous PTs, such as CdpNPT, have been applied to modify antibiotics, *e.g.*, daptomycin, improving bioactivity against resistant bacteria (Fig. 4).[46] In addition, CdpNPT's promiscuity and engineering enabled biorthogonal labelling of bioactive Trp-containing peptides, including alarelin and the FDA-approved drugs triptorelin and nafarelin. The non-natural alkenyl chain attached to alarelin (Fig. 4) allowed for subsequent click-chemistry of a tetrazine-biotin dye.[69] A similar approach was previously elaborated by Houssen and co-workers, using alkenyl donors, allowing for subsequent copper-catalysed azide–alkyne cycloaddition and inverse-electron-demand Diels–Alder reaction with fluorescein, using the cyanobactin PT AcyF, selective for Trp *N*-prenlyation.[58]

As mentioned above, there is a remarkable connection between the acceptor residue specificity of cyanobactin PTs and their tolerance for the surrounding peptide sequence. The resulting broad peptide substrate tolerance was used in library screening efforts with different representatives. The Schmidt lab used double- and quadruple-mutant libraries of *truE* encoded core peptide variants to produce more than 300 new compounds, including prenylated cyclic peptides, by heterologous co-production of the *tru* pathway in *Escherichia coli*.[70] Later, they utilized the macrocyclase PagG and the PT PagF to produce a library of more than 100 cyclic peptides and their prenylated derivatives *via* chemoenzymatic screening.[71] Recently, Inoue *et al.* used the highly promiscuous Trp PT KgpF, in combination with the RaPID platform, to produce a vast library of *C*-prenylated teMPs.[62] The library was screened against a potential anti-anthelmintic drug target, resulting in *de novo* drug design by taking advantage of the properties installed by peptide prenylation (Fig. 4).

PalQ and engineered variants thereof were very recently employed to prenylate AMPs with a C-terminal Trp (Fig. 4).[23] As

outlined above, the obtained prenylated peptides showed increased bioactivity over their non-prenylated counterparts, and an improved ratio between bioactivity and cytotoxicity, when compared with fatty acylated derivatives, demonstrating the translational potential of these enzymes.

5   Strategies for future biocatalyst discovery and optimization

Although numerous AA and peptide PTs have been characterised, and the field has advanced within the last decade, the chemical diversity is still far from being fully explored. Even though the AA acceptor residue diversity has increased recently with the characterization of Arg- and His-specific PTs, there are AA residues with nucleophilic potential that would allow for prenylation in the context of peptides, such as cysteine or lysine.[9,10,13,14,52,55] The first is a well-known target for protein prenylation, but the latter remains, to my knowledge, elusive.

SSNs generated for unique sequence-based homologs of the three main PT-folds discussed above (Fig. 2) – ABBA-fold PTs, IDS-like PTs, and terpene cyclase-fold PTs – highlight substantial untapped biosynthetic diversity (Fig. 5, SI).[72,73] Numerous clusters and subclusters in these SSNs lack any characterized members, and several large network clusters containing dozens to hundreds of unstudied PTs. Together, they point to a vast biosynthetic potential that could reveal new prenyl donor and acceptor specificities. Many of these clusters also contain representatives from talented but underexplored NP producers, such as cyanobacteria and myxobacteria, suggesting access to unprecedented NP scaffolds and new chemical entities.

The SSN of more than 2000 ABBA-fold PTs illustrates this untapped diversity. It was generated using the alignment score typically applied to generate chemoselective clusters of cyanobactin PTs. Cluster 1 contains TyrPT and SirD,[4,59] which catalyse *O*-prenylation of Tyr, as well as FunA,[9] which utilizes DMAPP for His *C*-prenylation. Although these enzymes fall into different subclusters, their grouping demonstrates the versatile chemoselectivity that can be uncovered from a single SSN cluster. Cluster 6 contains 88 uncharacterized NctP homologs, distinct from the native enzyme in cluster 20;[8] several of the NctP-like PTs are currently being investigated in the Hubrich lab. These two examples provide just a glimpse of the assumed biosynthetic potential hidden in the numerous clusters and singletons of uncharacterized bacterial and fungal ABBA-fold PTs.

A similar picture emerges from the SSN of 1644 IDS-like PTs. Clusters 1, 3, and 6 with 492, 220, and 96 nodes, respectively, contain no characterized representatives. Cluster 7 includes AgdS, AgdT, ScAer3, and GroH;[10,39] notably, GroH transfers a much longer prenyl donor and is not involved in NRP biosynthesis, unlike the other three enzymes. Finally, the SSN of 54 terpene cyclase-fold PTs contains only a single cluster with characterized enzymes, and all the representatives forming the cluster are algae and diatoms.[11] All remaining terpene cyclase-fold PT homologs form three clusters of bacterial and fungal enzymes and one moss singleton, again pointing to unexplored biosynthetic potential across multiple phyla.

The post-genomic era, in combination with the emerging power of artificial intelligence (AI) and machine learning (ML), provides new tools for genome mining with homology-based searches that overcome issues with low sequence similarity within and between different enzyme subfamilies. Foldseek is a first step in this direction, using an enzyme structure-based approach for the detection of homologs sharing the fold.[74] The ABBA-type PTs nicely exemplify the challenge that can be overcome with this approach. The overall fold of DMATS enzymes and cyanobactin PTs is highly similar, but shows distinct key features, likely responsible for differences in substrate scope, while the sequence identity is very low.[34] In addition, structural models of NctP-like PTs also show unique structural motifs and very low sequence similarity to DMATS and cyanobactin PTs, suggesting a distinct ABBA-type PT family.[8]

Another challenge of peptide PTs, especially in the context of RiPPs, is the reliable prediction of AA acceptor and/or prenyl donor specificity based on their AA sequence and predicted structure. Cyanobactin PT phylogenetically clade based on their chemoselectivity (Fig. 5), but sequence-based prediction of the utilized prenyl donor remains an unsolved challenge, despite the progress in switching donor specificity.[34,55,63] Computational predictions provide helpful support, but the number of experimental data points is not currently sufficient to support ML-based approaches. Here, the incorporation of 'negative' results from inactive PTs, together with the results obtained from other ABBA-type RiPP PTs, could help to increase the number of data points.

However, high-throughput screening (HTS) of peptide PTs must be considered not only as a strategy to generate more experimental data for AI/ML-assisted predictive modelling, but also to increase the limited number of characterized PTs. A so-far untapped opportunity relying on HTS is the directed evolution (DE) of peptide PTs.[75] DE provides access to more stable or active enzymes, expands or shifts substrate scope and donor specificity, while producing large numbers of experimental data points. Two major bottlenecks for HTS and DE of peptide PTs are the lack of suitable screening assays that provide inexpensive and rapid readouts and the cost-intensive pyrophosphate donors. The recently developed extended variant of a module for phosphate detection by UV-spectroscopic monitoring of bromouridine phosphorolysis (EPUB) showed promising results for pyrophosphate detection during chemoenzymatic prenylether synthesis.[76] In addition, newly developed platforms for *in silico* DE, such as *AI.zymes*, might significantly reduce the number of experimental data points that are required to evolve a specific PT, once a specific endpoint for optimization is defined.[77]

For other PTs, such as the IDS-like PT PalQ, structural modelling of precursor peptides with the PT guided the identification of the potential prenylation site at the C-terminal Trp.[57] Automated approaches along those lines might assist streamlined prioritization of RiPP pathways to detect unprecedented acceptor residues and prenyl donor combinations, especially when combined with the latest developments for AI-assisted structure prediction, incorporating small-molecule ligands, such as the beta version of Chai-1.[78]
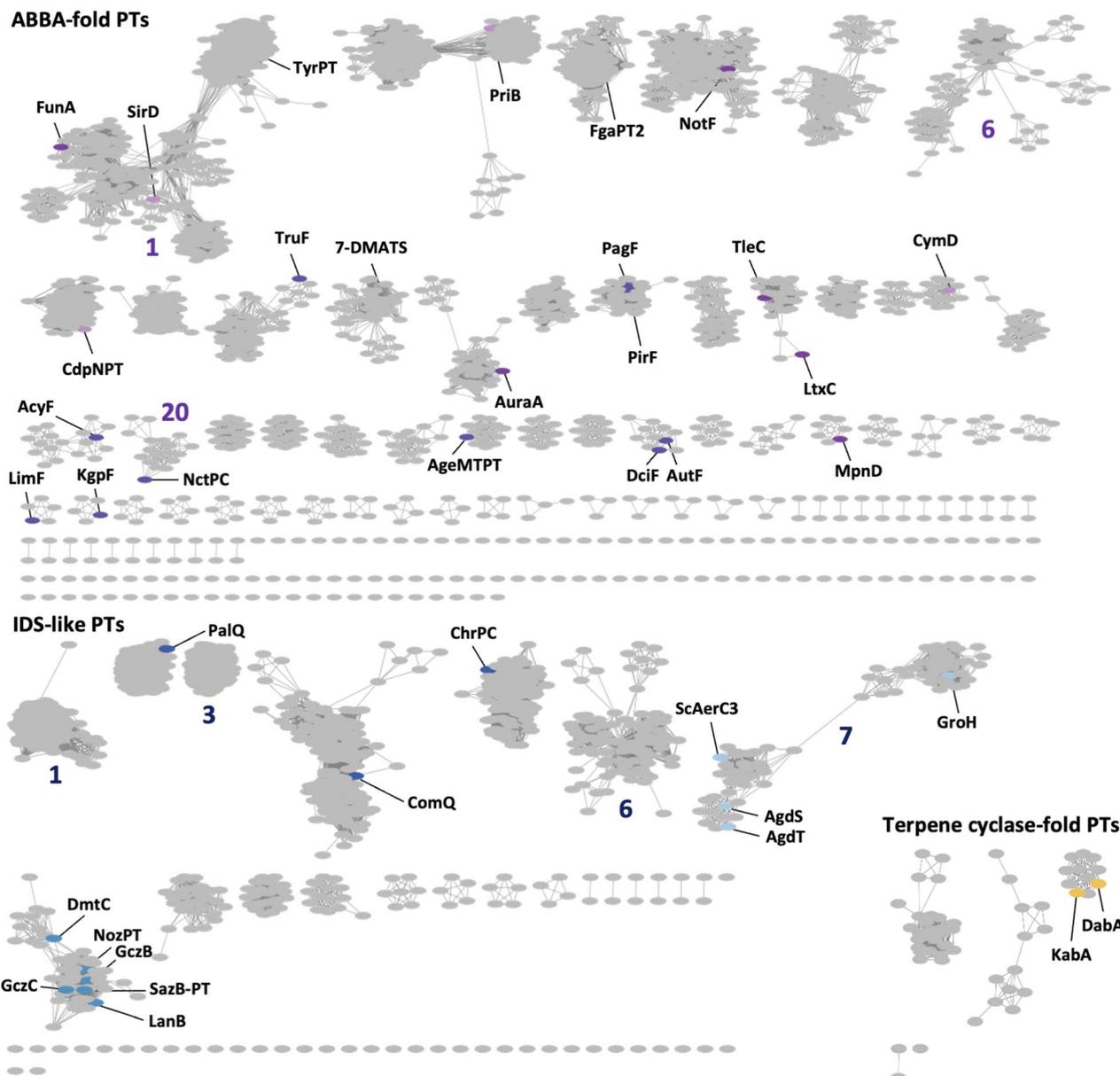
This journal is © The Royal Society of Chemistry 2026

Nat. Prod. Rep., 2026, **43**, 415–426 | **423**

Fig. 5 SSNs of ABBA-fold, IDS-like, and terpene cyclase-fold PTs generate with alignment scores of 85, 55, and 35, respectively. The ABBA-fold PTs are coloured in magenta for PTs with AA as native substrates, purple for PTs with DKPs and dipeptides as native substrates, and dark purple for PTs with RiPPs as native substrates. IDS-like PTs are coloured in grey blue for PTs with AA as native substrates, light blue for PTs with DKPs as native substrates, and dark blue for PTs with RiPPs as native substrates. Terpene cyclase-fold PTs are coloured in yellow. The purple and dark blue numbers below the clusters refer to the clusters discussed in the text.

Although the application of peptide PTs, such as PriB, PalQ or KgpF, highlights the value of PTs for peptide drug discovery pipelines, there is still limited knowledge of the general effects of peptide prenylation on bioactivity and bioavailability.[23,31,62] To establish a general understanding of the effects of peptide prenylation, systematic screenings of bioactive peptides with libraries of characterized PTs will be crucial. They will reveal the effects of distinct prenylated AAs within the same peptide chain, as well as the influence of different natural and non-natural prenyl donors at the same acceptor residue. The knowledge obtained from such systematic approaches will be used to harness the chemoenzymatic potential of peptide PTs and expand the biocatalytic PT toolbox. It will streamline the screening process for prenylated bioactive peptides, enable the large-scale production of specific prenylated building blocks for lipopeptide synthesis, and enable on-demand peptide late-stage functionalization during drug development.

6 Conflicts of interest

There are no conflicts to declare.

424 | *Nat. Prod. Rep.*, 2026, **43**, 415–426

This journal is © The Royal Society of Chemistry 2026

7 Data availability

All sequences of PTs, used as queries for homology-based searches, and all accession numbers of PTs, used to generate the SSNs, shown in Fig. 5 are provided in the supplementary information (SI). Supplementary information is available. See DOI: https://doi.org/10.1039/d5np00075k.

8 Acknowledgements

9 References

1 C. T. Walsh, *ACS Chem. Biol.*, 2014, **9**, 2718–2728.

2 C. C. Palsuledesai and M. D. Distefano, *ACS Chem. Biol.*, 2015, **10**, 51–62.

3 F. Hubrich, M. Müller and J. N. Andexer, *Chem. Commun.*, 2021, **57**, 2441–2463.

4 A. Kremer and S.-M. Li, *Microbiology*, 2010, **156**, 278–286.

5 A. W. Schultz, C. A. Lewis, M. R. Luzung, P. S. Baran and B. S. Moore, *J. Nat. Prod.*, 2010, **73**, 373–377.

6 M. S. Donia, J. Ravel and E. W. Schmidt, *Nat. Chem. Biol.*, 2008, **4**, 341–343.

7 S. P. Kelly, V. V. Shende, A. R. Flynn, Q. Dan, Y. Ye, J. L. Smith, S. Tsukamoto, M. S. Sigman and D. H. Sherman, *J. Am. Chem. Soc.*, 2022, **144**, 19326–19336.

8 F. Hubrich, S. K. Kandy, C. Chepkirui, C. Padhi, S. Mordhorst, P. Moosmann, T. Zhu, M. Gugger, J. R. Chekan and J. Piel, *Chem*, 2024, **10**, 3224–3242.

9 X.-W. Chen, Z. Liu, S. Dai and Y. Zou, *J. Am. Chem. Soc.*, 2024, **146**, 23686–23691.

10 W. Zhang, R. Ushimaru, M. Kanaida and I. Abe, *J. Am. Chem. Soc.*, 2025, **147**, 10853–10858.

11 J. R. Chekan, S. M. K. McKinnie, J. P. Noel and B. S. Moore, *Proc. Natl. Acad. Sci. U. S. A.*, 2020, **117**, 12799–12805.

12 J. A. McIntosh, Z. Lin, M. D. B. Tianero and E. W. Schmidt, *ACS Chem. Biol.*, 2013, **8**, 877–883.

13 W. Wang, P. Wang, C. Ma, K. Li, Z. Wang, Y. Liu, L. Wang, G. Zhang, Q. Che, T. Zhu, Y. Zhang and D. Li, *Nat. Commun.*, 2025, **16**, 144.

14 C.-S. Phan, K. Matsuda, N. Balloo, K. Fujita, T. Wakimoto and T. Okino, *J. Am. Chem. Soc.*, 2021, **143**, 10083–10087.

15 J. A. McIntosh, M. S. Donia, S. K. Nair and E. W. Schmidt, *J. Am. Chem. Soc.*, 2011, **133**, 13698–13705.

16 M. Purushothaman, S. Sarkar, M. Morita, M. Gugger, E. W. Schmidt and B. I. Morinaka, *Angew. Chem., Int. Ed.*, 2021, **60**, 8460–8465.

17 A. Mattila, R.-M. Andste2n, M. Jumppanen, M. Assante, J. Jokela, M. Wahlsten, K. M. Mikula, C. Sigindere, D. H. Kwak, M. Gugger, H. Koskela, K. Sivonen, X. Liu, J. Yli-Kauhaluoma, H. Iwaï and D. P. Fewer, *ACS Chem. Biol.*, 2019, **14**, 2683–2690.

18 C. C. Hanna, J. Kriegesmann, L. J. Dowman, C. F. W. Becker and R. J. Payne, *Angew. Chem., Int. Ed.*, 2022, **61**, e202111266.

19 A. K. Alexander and S. I. Elshahawi, *ChemBioChem*, 2023, **24**, e202300372.

20 J. R. Chekan, S. M. K. McKinnie, M. L. Moore, S. G. Poplawski, T. P. Michael and B. S. Moore, *Angew. Chem., Int. Ed.*, 2019, **58**, 8454–8457.

21 M. Muttenthaler, G. F. King, D. J. Adams and P. F. Alewood, *Nat. Rev. Drug Discovery*, 2021, **20**, 309–325.

22 H. Duan, M. Zhang, Z. Chen, X. Wang, F. Xiao and W. Li, *Bioorg. Chem.*, 2025, **160**, 108448.

23 H. Ozawa, A. Miyata, S. Hayashi, N. Miyoshi, K. Kato, S. Ito and D. Fujinami, *J. Am. Chem. Soc.*, 2025, **147**, 25642–25651.

24 C. Pancrace, K. Ishida, E. Briand, D. G. Pichi, A. R. Weiz, A. Guljamow, T. Scalvenzi, N. Sassoon, C. Hertweck, E. Dittmann and M. Gugger, *ACS Chem. Biol.*, 2019, **14**, 67–75.

25 U. Kazmaier and L. Junk, *Mar. Drugs*, 2021, **19**, 446.

26 L. Li, L. W. MacIntyre, T. Ali, R. Russo, B. Koirala, Y. Hernandez and S. F. Brady, *J. Nat. Prod.*, 2021, **84**, 1056–1066.

27 T. Mori, L. Zhang, T. Awakawa, S. Hoshino, M. Okada, H. Morita and I. Abe, *Nat. Commun.*, 2016, **7**, 10849.

28 X.-S. Yin, W.-Y. Qi and B.-F. Shi, *Chem. Sci.*, 2021, **12**, 13137–13143.

29 M. Okada, I. Sato, S. J. Cho, H. Iwata, T. Nishio, D. Dubnau and Y. Sakagami, *Nat. Chem. Biol.*, 2005, **1**, 23–24.

30 A. Kiefer, C. D. Bader, J. Held, A. Esser, J. Rybniker, M. Empting, R. Müller and U. Kazmaier, *Chem.–Eur. J.*, 2019, **25**, 8894–8902.

31 S. I. Elshahawi, H. Cao, K. A. Shaaban, L. V. Ponomareva, T. Subramanian, M. L. Farman, H. P. Spielmann, G. N. Phillips, J. S. Thorson and S. Singh, *Nat. Chem. Biol.*, 2017, **13**, 366–368.

32 L. C. Tarshis, M. Yan, C. D. Poulter and J. C. Sacchettini, *Biochemistry*, 1994, **33**, 10871–10877.

33 U. Metzger, C. Schall, G. Zocher, I. Unsöld, E. Stec, S.-M. Li, L. Heide and T. Stehle, *Proc. Natl. Acad. Sci. U. S. A.*, 2009, **106**, 14309–14314.

34 Y. Zhang, Y. Goto and H. Suga, *Trends Biochem. Sci.*, 2023, **48**, 360–374.

35 E. T. Miller, O. V. Tsodikov and S. Garneau-Tsodikova, *Nat. Prod. Rep.*, 2024, **41**, 113–147.

36 Y. Hao, E. Pierce, D. Roe, M. Morita, J. A. McIntosh, V. Agarwal, T. E. Cheatham, E. W. Schmidt and S. K. Nair, *Proc. Natl. Acad. Sci. U. S. A.*, 2016, **113**, 14037–14042.

37 A. Kremer, L. Westrich and S.-M. Li, *Microbiology*, 2007, **153**, 3409–3416.

38 A. Fan and S.-M. Li, *Appl. Microbiol. Biotechnol.*, 2016, **100**, 5389–5399.

39 S. Tistechok, D. Bratiichuk, H. Sucipto, N. Gummerlich, M. Stierhof, O. Gromyko, F. Fries, V. Fedorenko, R. Müller, J. Zapp, M. Myronovskyi and A. Luzhetskyy, *Angew. Chem., Int. Ed.*, 2025, **64**, e202422270.

40 T. Yao, J. Liu, Z. Liu, T. Li, H. Li, Q. Che, T. Zhu, D. Li, Q. Gu and W. Li, *Nat. Commun.*, 2018, **9**, 4091.

This journal is © The Royal Society of Chemistry 2026

Nat. Prod. Rep., 2026, **43**, 415–426 | **425**

41 G. Deletti, S. D. Green, C. Weber, K. N. Patterson, S. S. Joshi, T. M. Khopade, M. Coban, J. Veek-Wilson, T. R. Caulfield, R. Viswanathan and A. L. Lane, *Nat. Commun.*, 2023, **14**, 2558.

42 J. J. L. Malit, C. Wu, X. Tian, W. Liu, D. Huang, H. H.-Y. Sung, L.-L. Liu, I. D. Williams and P.-Y. Qian, *Org. Lett.*, 2022, **24**, 2967–2972.

43 Y. Zhang, T. Yao, Y. Jiang, H. Li, W. Yuan and W. Li, *Appl. Environ. Microbiol.*, 2021, **87**, e02525–20.

44 A. Fan, J. Winkelblech and S.-M. Li, *Appl. Microbiol. Biotechnol.*, 2015, **99**, 7399–7415.

45 J. Winkelblech, A. Fan and S.-M. Li, *Appl. Microbiol. Biotechnol.*, 2015, **99**, 7379–7397.

46 E. M. Scull, C. Bandari, B. P. Johnson, E. D. Gardner, M. Tonelli, J. You, R. H. Cichewicz and S. Singh, *Appl. Microbiol. Biotechnol.*, 2020, **104**, 7853–7865.

47 X. Yu, C. Ma, W. Wang, J. Ge, Z. Wang, J. Lin, Q. Che, G. Zhang, T. Zhu and D. Li, *Org. Lett.*, 2024, **26**, 3349–3354.

48 D. Richter and J. Piel, *Curr. Opin. Chem. Biol.*, 2024, **80**, 102463.

49 M. Morita, Y. Hao, J. K. Jokela, D. Sardar, Z. Lin, K. Sivonen, S. K. Nair and E. W. Schmidt, *J. Am. Chem. Soc.*, 2018, **140**, 6044–6048.

50 A. Parajuli, D. H. Kwak, L. Dalponte, N. Leikoski, T. Galica, U. Umeobika, L. Trembleau, A. Bent, K. Sivonen, M. Wahlsten, H. Wang, E. Rizzi, G. De Bellis, J. Naismith, M. Jaspars, X. Liu, W. Houssen and D. P. Fewer, *Angew. Chem., Int. Ed.*, 2016, **55**, 3596–3599.

51 L. Dalponte, A. Parajuli, E. Younger, A. Mattila, J. Jokela, M. Wahlsten, N. Leikoski, K. Sivonen, S. A. Jarmusch, W. E. Houssen and D. P. Fewer, *Biochemistry*, 2018, **57**, 6860–6867.

52 Y. Zhang, K. Hamada, D. T. Nguyen, S. Inoue, M. Satake, S. Kobayashi, C. Okada, K. Ogata, M. Okada, T. Sengoku, Y. Goto and H. Suga, *Nat. Catal.*, 2022, **5**, 682–693.

53 Y. Zheng, Y. Cong, E. W. Schmidt and S. K. Nair, *Acc. Chem. Res.*, 2022, **55**, 1313–1323.

54 Y. Zhang, Y. Goto and H. Suga, *Trends Biochem. Sci.*, 2023, **48**, 360–374.

55 D. Sardar, Y. Hao, Z. Lin, M. Morita, S. K. Nair and E. W. Schmidt, *J. Am. Chem. Soc.*, 2017, **139**, 2884–2887.

56 K. Fujita, Y. Yamada, T. Taniguchi, D. Fujinami, T. Mori, K. Matsuda, I. Abe and T. Wakimoto, *J. Am. Chem. Soc.*, 2025, **147**, 24766–24773.

57 F. Tsuji, A. Ishihara, A. Nakagawa, M. Okada, S. Kitamura, K. Kanamura, Y. Masuda, K. Murakami, K. Irie and Y. Sakagami, *Biosci., Biotechnol., Biochem.*, 2012, **76**, 1492–1496.

58 A. Miyata, S. Ito and D. Fujinami, *Adv. Sci.*, 2024, **11**, 2307372.

59 A. Colombano, L. Dalponte, S. Dall'Angelo, C. Clemente, M. Idress, A. Ghazal and W. E. Houssen, *Angew. Chem., Int. Ed.*, 2023, **62**, e202215979.

60 H.-X. Zou, X. Xie, X.-D. Zheng and S.-M. Li, *Appl. Microbiol. Biotechnol.*, 2011, **89**, 1443–1451.

61 D. A. Dimas, V. Kumar, P. S. Mandal, J. M. Masterson, M. Tonelli and S. Singh, *ChemBioChem*, 2024, **25**, e202400503.

62 S. Inoue, D. T. Nguyen, K. Hamada, R. Okuma, C. Okada, M. Okada, I. Abe, T. Sengoku, Y. Goto and H. Suga, *Angew. Chem., Int. Ed.*, 2024, **63**, e202409973.

63 Y. Zhang, K. Hamada, M. Satake, T. Sengoku, Y. Goto and H. Suga, *J. Am. Chem. Soc.*, 2023, **145**, 23893–23898.

64 L. Zheng, P. Mai, A. Fan and S.-M. Li, *Org. Biomol. Chem.*, 2018, **16**, 6688–6694.

65 Y. Zhang, Y. Goto and H. Suga, *Israel J. Chem.*, 2024, **64**, e202300182.

66 Y. Cong, P. D. Scesa and E. W. Schmidt, *ACS Synth. Biol.*, 2022, **11**, 3699–3705.

67 P. Mai, G. Zocher, T. Stehle and S.-M. Li, *Org. Biomol. Chem.*, 2018, **16**, 7461–7469.

68 P. Estrada, M. Morita, Y. Hao, E. W. Schmidt and S. K. Nair, *J. Am. Chem. Soc.*, 2018, **140**, 8124–8127.

69 N. Mupparapu, B. Syed, D. N. Nguyen, T. H. Vo, A. Trujillo and S. I. Elshahawi, *Org. Lett.*, 2024, **26**, 2489–2494.

70 D. E. Ruffner, E. W. Schmidt and J. R. Heemstra, *ACS Synth. Biol.*, 2015, **4**, 482–492.

71 S. Sarkar, W. Gu and E. W. Schmidt, *ACS Catal.*, 2020, **10**, 7146–7153.

72 S. F. Altschul, T. L. Madden, A. A. Schäffer, J. Zhang, Z. Zhang, W. Miller and D. J. Lipman, *Nucleic Acids Res.*, 1997, **25**, 3389–3402.

73 R. Zallot, N. Oberg and J. A. Gerlt, *Biochemistry*, 2019, **58**, 4169–4182.

74 M. van Kempen, S. S. Kim, C. Tumescheit, M. Mirdita, J. Lee, C. L. M. Gilchrist, J. Söding and M. Steinegger, *Nat. Biotechnol.*, 2023, **42**, 243–246.

75 K. K. Yang, Z. Wu and F. H. Arnold, *Nat. Methods*, 2019, **16**, 687–694.

76 F. Kaspar, L. Eilert, S. Staar, S. W. Oung, M. Wolter, C. S. G. Ganskow, S. Kemper, P. Klahn, C. R. Jacob, W. Blankenfeldt and A. Schallmey, *Angew. Chem., Int. Ed.*, 2024, **63**, e202412597.

77 L. P. Merlicek, J. Neumann, A. Lear, V. Degiorgi, M. M. de Waal, T.-S. Cotet, A. J. Mulholland and H. A. Bunzel, *Angew. Chem., Int. Ed.*, 2025, **64**, e202507031.

78 C. D. Team, J. Boitreaud, J. Dent, M. McPartlon, J. Meier, V. Reis, A. Rogozhonikov and K. Wu, *bioRxiv*, 2024, preprint, DOI: 10.1101/2024.10.10.615955.

426 | *Nat. Prod. Rep.*, 2026, **43**, 415–426

This journal is © The Royal Society of Chemistry 2026